Master's Programme in [Clinical Research Centre]

Nanoscale detection of insulin granule sub-structures using dSTORM imaging

by

[Yu Hong yu4072ho-s@student.lu.se]

LUND UNIVERSITY

Master's Thesis (60 credits ECTS)
(Sep) (2019)
Supervisor: [Enming Zhang]
Co-supervisor:[Cord Arnold]

Abstract

Diabetes mellitus is a global disease, mainly caused by insufficient insulin secretion from pancreatic islet β-cells. Insulin is stored in the granules of islet β-cells and released in response to extracellular stimuli e.g. glucose. The state of insulin structure and maturation determines the quality of the released insulin, However, the insulin state in the granules is rarely investigated due to lack of proper methods.

Here, we hypothesize that high-resolution microscopy and appropriate image analysis methods could be used to detect the insulin state in the granule. We used direct stochastic optical reconstruction microscopy (dSTORM), which is a super-resolution imaging method, to capture cellular insulin granules images and obtain the location of insulin molecules labelled by an insulin single-domain fluorescent antibody. The images were processed by the optimized algorithm of layering and filtering until the clusters of fluorescent dots in the images were distinguished. Then the hypothetical structures were used to scan the images to find the complete hexamer. In summary, this study provides novel method to study mature insulin crystals in the granular of islet β-cells.

Contents

1

Introduction

Diabetes, as a global medical problem, is a metabolic disease, which causes angiocardiopathy, strokes and other complications. According to the World Health Organization, an estimated 422 million people worldwide had diabetes in 2014 [1]. Most type-2 diabetes are associated with insufficient insulin secretion from pancreatic islet β-cells. Insulin stored in insulin granules in the cell determines the amounts of insulin secretion in response to blood glucose. Therefore, the detection of the substructure of insulin granule is vital to understand the mechanism of insulin secretion insufficiency.

The chemical structure of insulin has been detected previously. In 1969, Dorothy Hodgkin determined the 3D structure of insulin crystals using X-ray crystallography [2]. Later, laboratories around the world used different methods, such as Nuclear Magnetic Resonance spectroscopy (NMR) [6], Electron Paramagnetic Resonance(EPR) [18], to figure out the spatial structure of insulin.

However, the detection of insulin state and its sub-structure in insulin granule remains elusive, especially how the insulin transfers to the state of mature solid crystals synthesized in vitro [2]. The structure and synthesis process of insulin structure within cells are incredibly complicated and unknown. To analyze the structure or distribution of insulin in islet β-cells directly, we employed the Stochastic Optical Reconstruction Microscopy (STORM) imaging technology [14], to capture the super-resolution images of the cells. Due to the positional information of a single fluorescent molecule obtained directly, we found that dSTORM imaging is a suitable way to analyze sub-structures in the cells.

We have labelled insulin cells with Alexa Fluor 647 conjugated single-domain insulin antibody [11]. Then we used the ELYRA P1 microscope to acquire the image of islet β-cells, which obtained the position information of the insulin molecules [21]. We extracted the organelle data (granule) from the entire cell image for analysis.

In summary, this thesis shows four main methods to analyze the image data, stated in section 4, and also found distinct clusters in these sub-cellular images, and some basic structure can be parsed out in the clusters, which indicates that these clusters may represent an individual cell behaviour.

2

Theory

2.1 Blood glucose regulation mechanism

Insulin is a protein hormone secreted by islet β-cells in the pancreas. Its function is to prompt the liver and skeletal muscles to convert glucose into glycogen in the blood. It regulates the carbohydrate and fat metabolism and controls the balance of blood glucose. An inefficient insulin processing can lead to high blood sugar and in severe cases to diabetes. Figure 2.1 illustrates the mechanism of insulin regulation.

When glucose concentration is elevated in the blood, it causes the islet β-cells of the pancreas to secrete large amounts of insulin crystals. The insulin crystals are transmitted through the blood to the liver, skeletal muscles, fat cells, and so on, which are promoted to absorb glucose from the blood and convert it to glycogen or fat for storage. Moreover, insulin also inhibits the degradation of fat and the synthesis of glucose. Both of these ways, insulin decreases glucose concentration and plays a role in maintaining glucose concentration balance [4].

There are three main types of diabetes [12]:

- **Diabetes type 1:** caused by no or little insulin produced by the pancreas.
- **Diabetes type 2:** caused by relatively insufficient insulin produced by islet β-cells in the setting of insulin resistance.
- **Gestational diabetes:** cause unknown.

Diabetes type 2 accounts for 85 to 90 percent of all cases worldwide. The common reason for type 1 and 2 is insufficient insulin produced by islet β-cells [3]. Therefore, studying the physiological behaviour of insulin crystals in islet β-cells is beneficial to the understanding of diabetes.

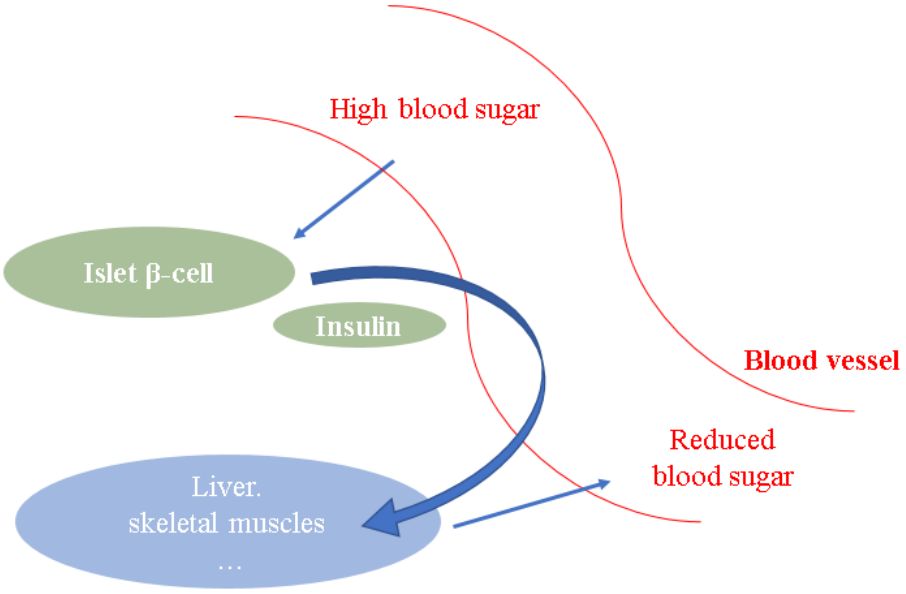

Figure 2.1: The figure shows the mechanism of insulin regulation.

2.2 The composition and structure of insulin

Mature insulin crystals are known by their structure as insulin hexamers [7]. Each insulin hexamer is composed of three dimers that are combined by two zinc ions and one calcium ion to form a stable insulin hexamer structure [19]. Figure 2.2 illustrates the structure of the insulin hexamer. The insulin dimer is composed of intertwining two peptide chain A and peptide chain B, see Figure 2.2(a). The A chain of human insulin contains 11 kinds of 21 amino acids, and the B chain contains 15 kinds of 30 amino acids, both of them called insulin monomer [8].

The three-dimensional structure of the insulin crystal has been studied using different technologies during the 20^{th} century. In 1969, Dorothy Hodgkin determined the three-dimensional structure of solid insulin with X-ray crystallography. In her work, the mature solid insulin crystals were synthesized in vitro. Due to the diffraction of the crystal obeying Laue and Bragg equations, the crystal density map can be reconstructed. Finally, the three-dimensional structure of the insulin crystal is constructed from the crystal density map [2].

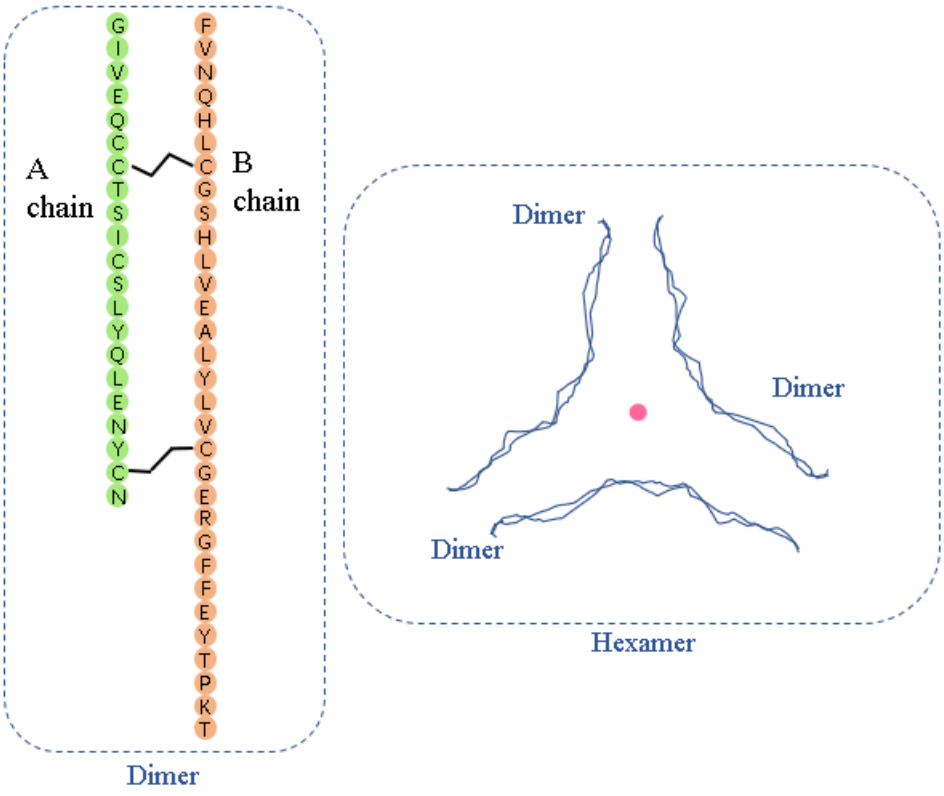

Figure 2.2: The image (b) illustrates the sketch structure of the insulin hexamer. One dimer for every third, which consists of chain A and B, illustrated in image (a). The intermediate molecule (pink circle) is zinc ion [20].

2.3 The processing of insulin in the granule

Insulin crystals are secreted by islet β-cells. Moreover, the insulin crystals are produced and stored in granules within the islet β-cells. Each islet β-cell has an average of 10,000 granules. Each granule contains about 200,000 insulin monomers. The granule is an organelle, whose size is 200 to 300 nm [15], which is shown in Figure 2.3.

However, the synthesis of insulin in cells is complicated, and the brief description is as follows and is illustrated in Figure 2.4:

- Islet β-cell first produces preproinsulin containing 102 amino acids in the rough endoplasmic reticulum (Step 1). When preproinsulin passing through the endoplasmic reticulum membrane, Preproinsulin cuts off the 16 amino acid leader sequence into proinsulin, containing 86 amino acids. The proinsulin is transported into the granule. In the granules, by the action of proteolytic enzymes, proinsulin is cleaved into three chains, including the inactive C chain, A chain and B chain (Step 2). The spatial structure of A chain and B chain is further modified to form a dimer(Step 3). Finally, the three dimers are connected to form an insulin hexamer [15].

Electron microscope has a very high resolution image of the cell, but the principle is based on the electron density which means we can not analyse the sub-structure

in the granule. This is why we used the new technology "dSTORM" to explore the sub-structure in the cells. However, the dSTORM images we took may contain not only the position information of the stable and mature insulin hexamer but also of the dimer being processed, which complicates the image information and makes the task more challenging.

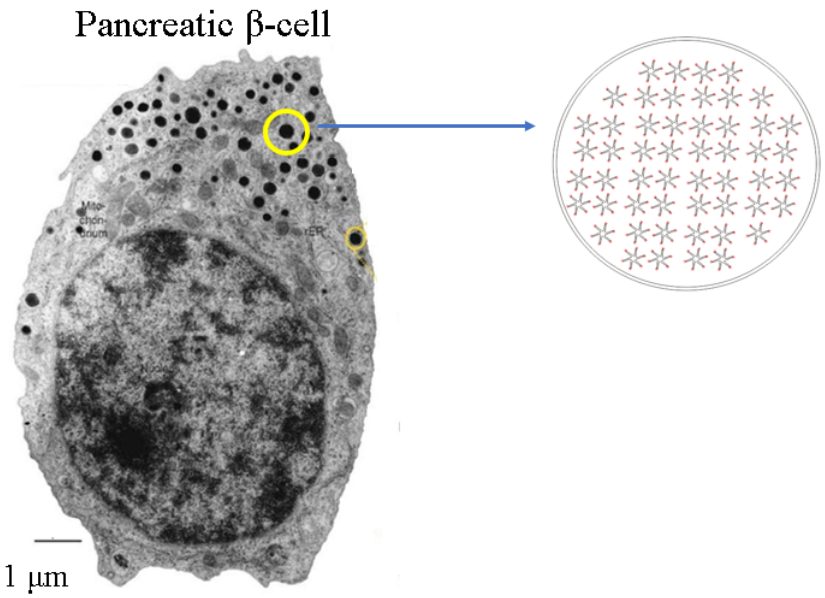

Figure 2.3: The cell diagram is the original electron microscope image.The yellow circle is granule. Granule is full of insulin monomers. Adapted from the figure in the bibliography [15].

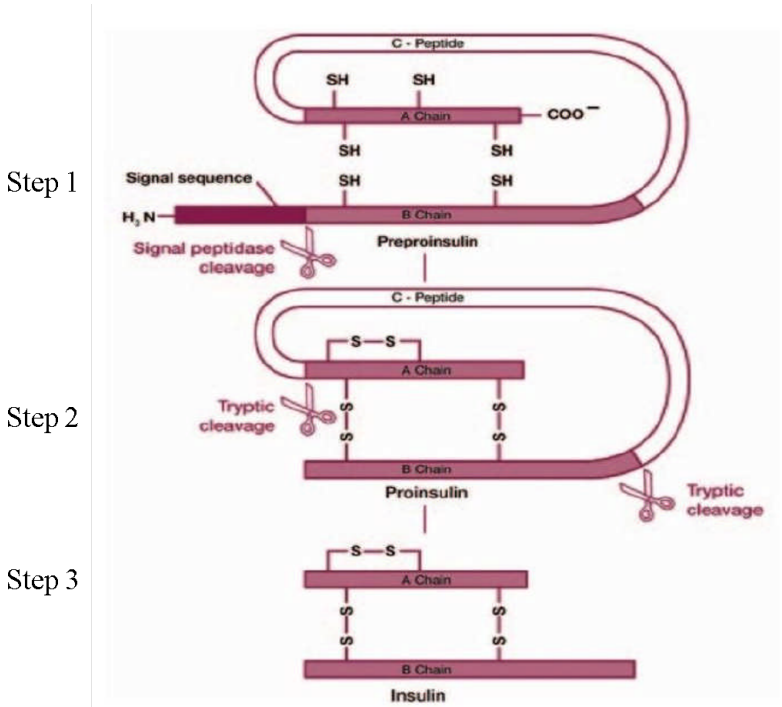

Figure 2.4: The schematic diagram of the synthesis of insulin. Adapted from the figure in the bibliography[10].

2.4 The structure of insulin combined with dye and protein

As stated in section 2.5, dSTORM is a single molecule fluorescence technique. Moreover, the fluorescent molecule is not an insulin crystal, but a dye fluorescent molecule. The dye fluorescent molecule is combined with the insulin monomer by a specific protein. Based on introduction of the insulin structure in section 2.2, Figure 2.5 illustrates a simplified model of the insulin hexamer as a sample, which is the structure we have predicted. Each monomer is combined with a dye molecule. The fluorescence location obtained directly represents the position of the dye molecule, which means that it indirectly indicates the location of the insulin monomer. The hexagon on the right of Figure 2.5 is a further simplified structure as the basic model in our analysis of the images later. The structure of other structures in cells such as dimers cannot be reasonably predicted due to the complexity of the organism. In this experiment, the dye we use is Alexa Fluor 647 (Section.2.6, which lead to that the size of the hexagon can be predicted in Figure 2.5.

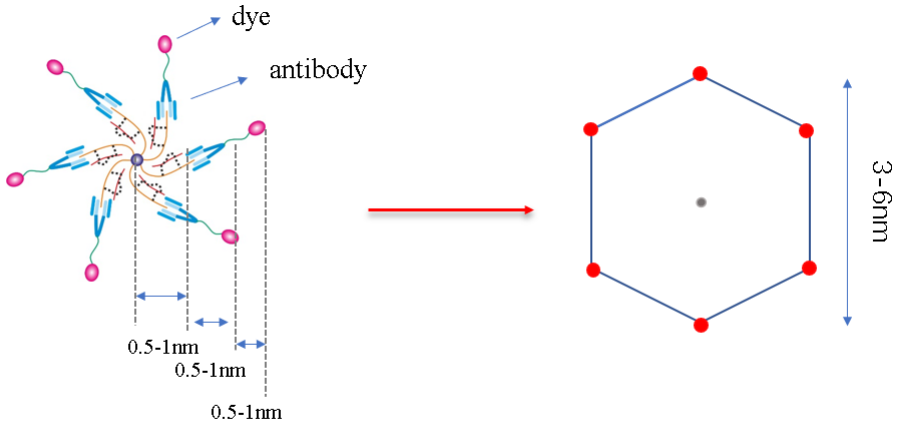

Figure 2.5: The schematic diagram of the structure of insulin combined with dye and protein.

2.5 Single molecule fluorescence

dSTORM is a single molecule fluorescence technique, which is that the position of the dye molecule is determined by the fluorescent signal of the dye molecules. The principle is illustrated in Figure 2.6. After the molecule absorbs a photon supplied by a laser, it is excited from S_0 to S_1 or S_n, and then decays to the lowest vibrational level of S_1 or S_n by vibrational relax, when is non-radiation.

Next step, the molecule has two major ways of decay back to the ground state.

- A fluorescent photon is emitted. The fluorescence decay time is very short about 10^{-8}s, which indicates that when the dSTORM image is capturing, it is burst out in the form of a blink, which is recorded by the by Electron Multiplying Charge Coupled Devise(EMCCD). This blink image is also the primary data for locating the position of the molecule. As the schematic 2.6 illustrates that the difference between the laser wavelength and the fluorescence wavelength, which make the collected information more reliable and avoid the interference of the laser.

- The another way, through the inter-system crossing, the excited dye molecule will transmit to the triplet state, and then decay to group state by emitting a phosphorescent photon. The decay time of phosphorescence is longer (10^{-0}s-10^{-3}s). When we are collecting images, there are a lot of bright spots lasting a long time, which will be automatically filtered out by the microscope software.

Figure 2.6 shows the principle of the single molecule fluorescence which is the basis of dSTORM microscopy [16].

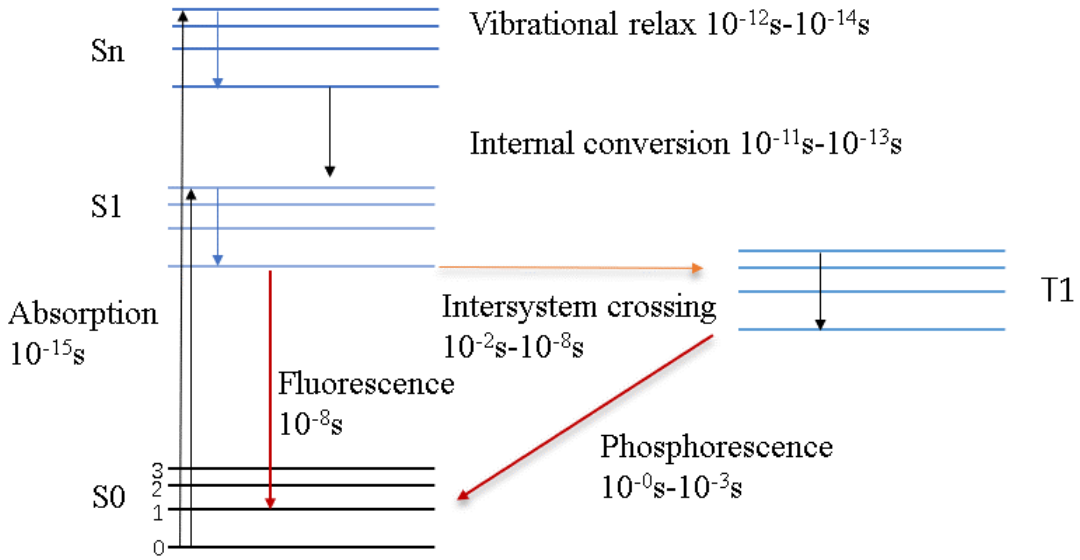

Figure 2.6: The principle of single molecule fluorescence. S_0 is the ground state, S_1 is the first excited singlet state, and Sn is the high-order excited singlet state. T_1 is the excited triplet state [16].

2.6 Alexa Fluor 647

For some dye molecules, such as the Cy3-Cy5 dye pair, two different wavelengths of laser are needed to realize state transition. Alexa Fluor 647 is a fluorescent molecule that automatically switches between excited state and dark state instead of two lasers control. Because the rate at which a dark state turns into a excited state is very low, only a small number of fluorescent molecules are in the excited state at the same time. This optical characteristic is the basis of single molecule localization imaging. In conjunction with the imaging buffer, the lifetime of the excited state is controlled, which makes the Alexa Fluor 647 ideal for dSTORM imaging. Fluorescence spectrum of Alexa Fluor 647 is shown in Figure 2.7. The excitation peak is 651 nm and emission peak is 667 nm. At 641 nm, its value is 91 % of the peak value, which means that this wavelength laser is suitable for the experiment.

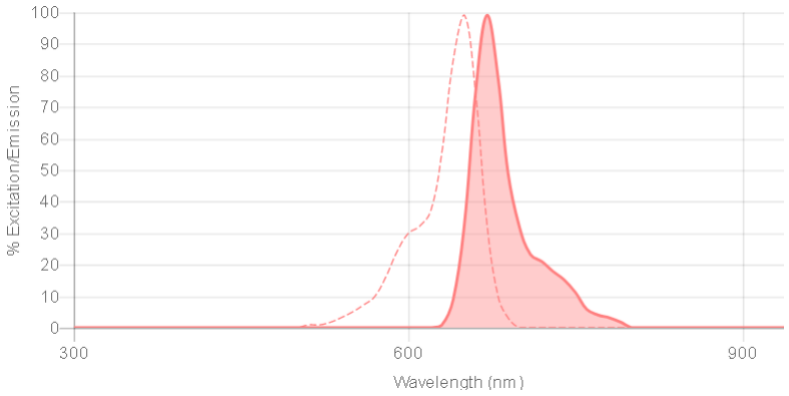

Figure 2.7: The excitation and emission spectrum of Alexa Fluor 647. The dotted line indicates the excitation spectrum and the solid line indicates the emission spectrum [11].

2.7 Direct Stochastic Optical Reconstruction Microscopy

2.7.1 The physical principle of dSTORM

Direct Stochastic Optical Reconstruction Microscopy (dSTORM) is a super-resolution microscopy technology, which was proposed by Harvard professor Xiaowei Zhuang in 2006 [14]. A similar technology proposed in the same year is Photo-activated localization microscopy (PALM)[5]. Both of them are single-molecule localization techniques.

The resolution of conventional microscopy is limited by the Abbe diffraction limit. In order to obtain a higher resolution, the fluorescence microscope was come up, such as laser confocal scanning microscopy (LCSM) [13]. Conventional fluorescence microscopy uses different fluorescent molecules to label different parts of the sample such as organelles. Moreover, the images are taken by detecting the fluorescence of dye molecules.

However, for conventional fluorescence microscopy, the process that fluorescent molecules emit fluorescence is uncontrollable. All fluorescent molecules that are exposed by a specific laser will emit fluorescence. For example, as illustrated in the image D1 of Figure 2.8, all molecules in the "LUND" letter image will be excited at the same time, which causes the image to appear blurred.

For the dSTORM technology, special fluorescent dyes are used, which can be switched between the fluorescence excited state and dark state by the illumination of two different laser wavelengths [14]. The process of fluorescing in such fluorescent dye molecules is controllable. In a very short time (50 ms), only a small amount of dye molecules are turned to the excited state. By laser excitation, these dye molecules emit fluorescence to obtain a frame, such as the image D2 of Figure 2.8. Each frame contains the positional information of a small fraction of the dye molecules. Different dye molecules are statistically turned on and off. At any time, only a small number of dye molecules is in the active state. The above process is repeated to get thousands of frames and finally, all frames are superimposed to reconstruct a super-resolution image, such as the image D3 of Figure 2.8. It should be noted that the microscope software has to perform a number of complicated statistical analysis and correction tasks, such as filtering of multiple counts for molecules that have been in the on-state several times.

2.7.2 Location algorithm of dSTORM

In each frame, the fluorescence signal of each fluorescent molecule is recorded by EMCCD and illustrated in Figure 2.9. Each pixel contains the number of recorded photons. As illustrated in the image C of Figure 2.9, the centre position of the single-molecule fluorescence is located by fitting the Gaussian function [9]

$$I(x_c, y_C, A, B) = \frac{A}{2\pi\sigma_x\sigma_y} exp(-\frac{(x-x_c)^2}{2\sigma_x^2} - \frac{(y-y_c)^2}{2{\sigma_y}^2}) + B \tag{2.1}$$

where the σ_x and σ_y are the standard deviations, (x_c, y_c) is the coordinates of the center, A is the amplitude corresponding to the number of recorded photons and B is the background signal.

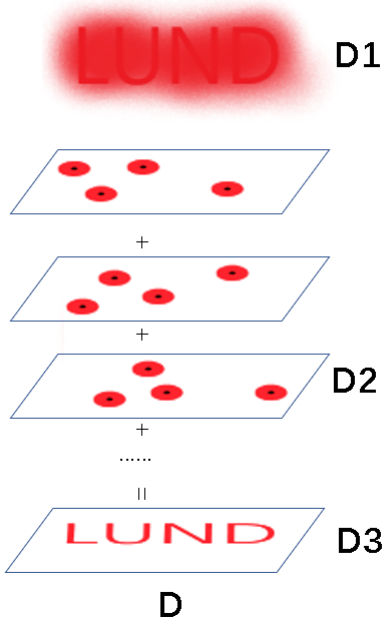

Figure 2.8: The principle of Direct Stochastic Optical Reconstruction Microscopy (dSTORM).

The approximate formula for its position in two-dimensional localization precision is [17]

$$(\Delta x) = \sqrt{\frac{s^2 + \frac{a^2}{12}}{N} + \frac{8\sqrt{\pi}s^4 b^2}{a^2 N^2}} \tag{2.2}$$

where Δx is the error in localization, N is the number of photons collected, s is the radius of the point spread function(PSF) (typical about $150nm$), a is the size of the pixels (100 nm) and b^2 is the background noise (typical < 100) . Based on this equation, the higher the number of photons collected, the higher the accuracy. For example, if the number of the photons for each dye molecule is lager than 10,000, the horizontal localization precision (x-y) is about $10nm$.

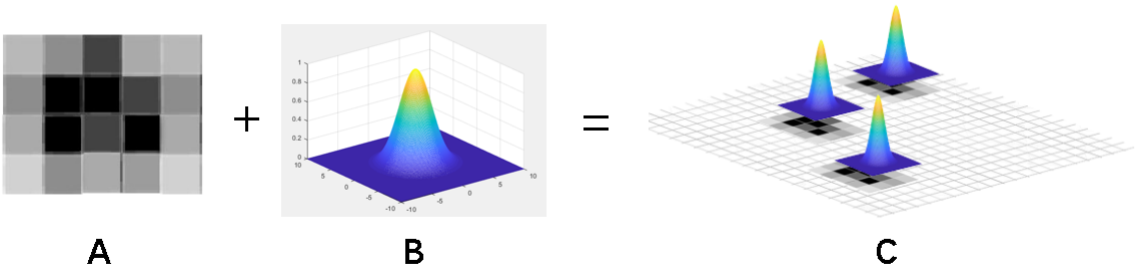

Figure 2.9: The method of dSTORM single molecular location.

In order to achieve high resolution in the Z-axis, a cylindrical mirror was added to the imaging system. The astigmatism caused by the cylindrical lens makes the positioning function become an elliptical point spread function. The length and direction of the long axis of the ellipse contain the axial information of the molecule, shown in Figure 2.10. The point spread function can still be represented by the

function 2.2. And the relationship between the Z axis position and the (σ_x, σ_y) is [9]

$$\sigma_{x,y} = \sigma_0 \sqrt{1 + (\frac{z-c}{d})^2 + A(\frac{z-c}{d})^3 + B(\frac{z-c}{d})^4} \tag{2.3}$$

where σ_0 is the PSF radius when the molecule is at the focal plane, d is the focus depth of the microscope, c is the offset of the x or y focal plane, and A and B are coefficients of higher order terms to correct for the non-ideality of the imaging optics. By using it, the Z axis position of the fluorescent molecule can be determined. The localization precision on the z-axis is about 50 nm with this approach.

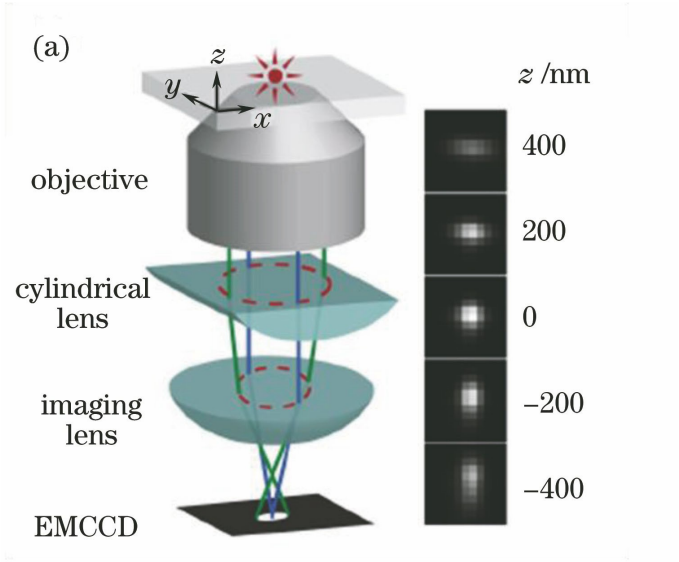

Figure 2.10: Schematic diagram of fluorescence molecular shape change for different focal depth when a cylindrical mirror is added to the imaging path. The figure was reproduced from [9].

3

Setup and Sample Preparation

3.1 The Setup of dSTORM

In this study, Zeiss company ELYRA P1 microscopy system is used for all experiments, shown in Fig.3.1. The schematic beam path of ZEISS Elyra P1 can be found on the official website. Here we simplified the beam path, which is illustrated in Figure 3.1.

The setup is installed with four different excitation laser lines. In this project, the 640nm diode laser with 150 mW output was used. The laser beam is expanded through the optical system and then focused to the specimen through the objective lens to excite Alexa Fluor 647 dye. The fluorescent signal was recorded by Electron Multiplying Charge Coupled Device (EMCCD). EMCCD is a sensor capable of detecting a single photon event without an image intensifier, which can be realized by a unique electron multiplication structure built into the chip. It has characteristics of high sensitivity and high speed, which is used usually in single molecule detection technology. Andor iXon 897 back-thinned EMCCD camera is used in the microscopy.

In front of the EMCCD, the optical filter was used to block the light (<641 nm) which maximum sensitivity for the signal and reduce background noise.

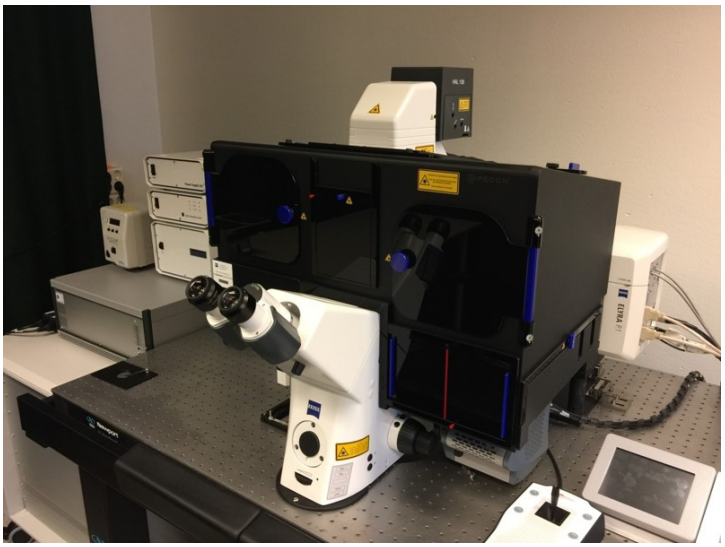

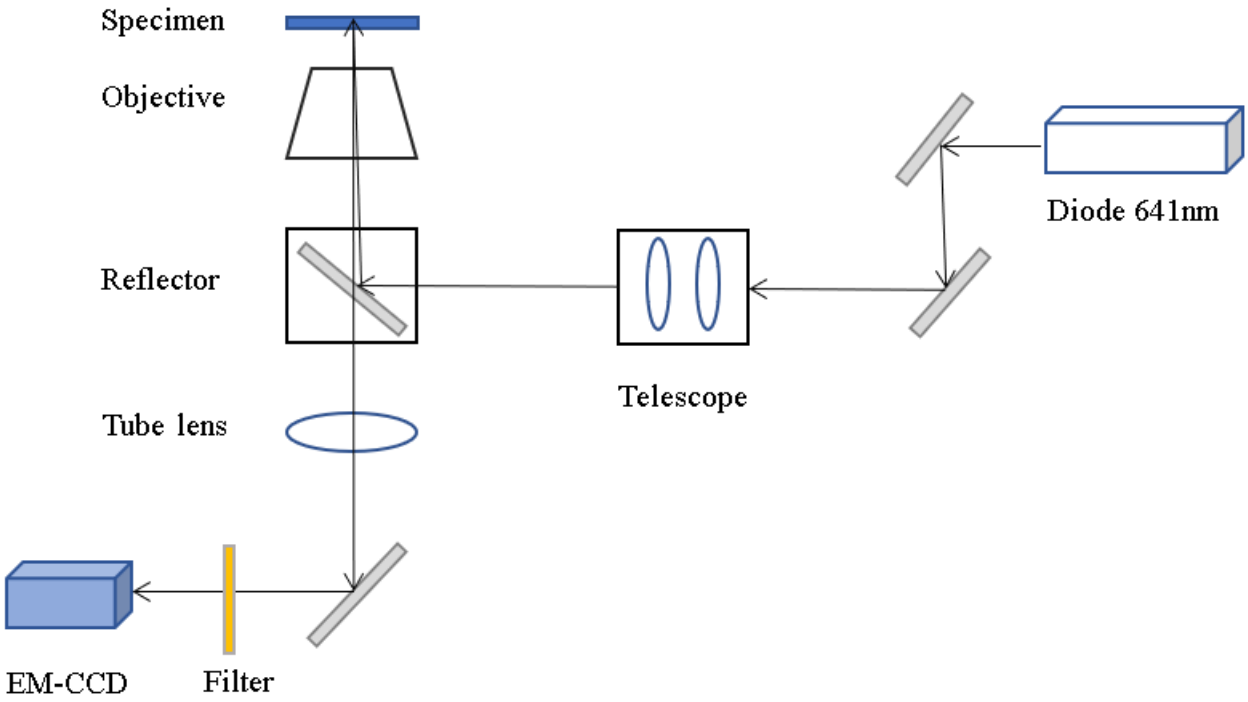

Figure 3.1: The microscopy of ZEISS Elyra P1 and its simplified schematic beam path [21].

3.2 Sample preparation

The description of the sample preparation and illustrated in Figure 3.2 :

- Cell culture: The 100K islet β-cells were seeded in a glass bottle.
- Cells were fixed using phosphate buffered saline (PBS) with 3% paraformaldehyde and 0.1% glutaraldehyde for ten minutes. Then the immunostaining of insulin is performed by addition of a single domain antibody (1:2000 dilution) tagged with Alexa Fluor 647.
- Before the cell imaging, it is necessary to add imaging buffer. Imaging buffer is used to regulate the opening frequency of fluorescent dye molecules. Alexa

Fluor 647 dye is a dye that can automatically switch between the excited and dark state. In our experiments, only a laser with a wavelength of 641 nm is required to excite the fluorescence instead of the two lasers. By using the imaging buffer, the fluorescent molecules have a longer lifetime in the excited state, to obtain enough photons and improve the localization precision. In the experiment, the imaging buffer contained 50 mM Tris, 10 mM NaCl, 0.5 mg/mL glucose oxidase, 40 g/mL catalase, 10% (w/v) glucose and 1% (v/v) -Mercaptoethanol [9].

- Finally, due to the thin glass in the middle of the bottle, the buffer-treated sample can be imaged directly by the dSTORM microscopy.

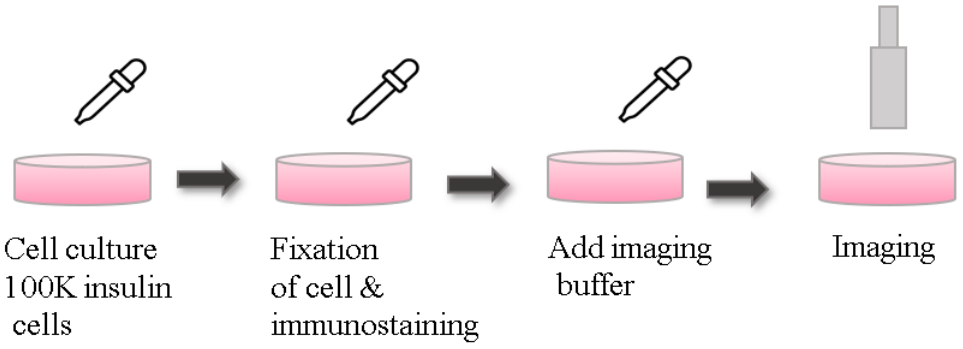

Figure 3.2: The simplified schematic diagram for the sample preparation.

4

Methods

4.1 Layering process

In order to study the substructure in a granule, preprocessing of the dSTORM data is necessary. As shown leftmost (A) in Figure 4.1, a dSTORM image is a superposition of a series of frames, which were taken about over a time of 5 minutes. The density of the fluorescent spots in the final image is extremely high, which is not convenient for our analysis of substructures. A dSTORM image is usually a superposition of more than 10,000 frames. Based on this, we can divide it into sub-images which contain several hundred frames each. This process is named Layering, shown in Figure 4.1. The idea is to select an appropriate number of frames to construct an image with less fluorescent points (as compared to the full image), which is easier to analyse.

In terms of time, it is equivalent to an image acquired in a shorter time, and the relative position of the spots is more stable and credible. The selection range is flexible rather than limited by the definition of the microscope system. In this way, it is the basis for analyzing structures that are smaller, such as a few nanometers structure.

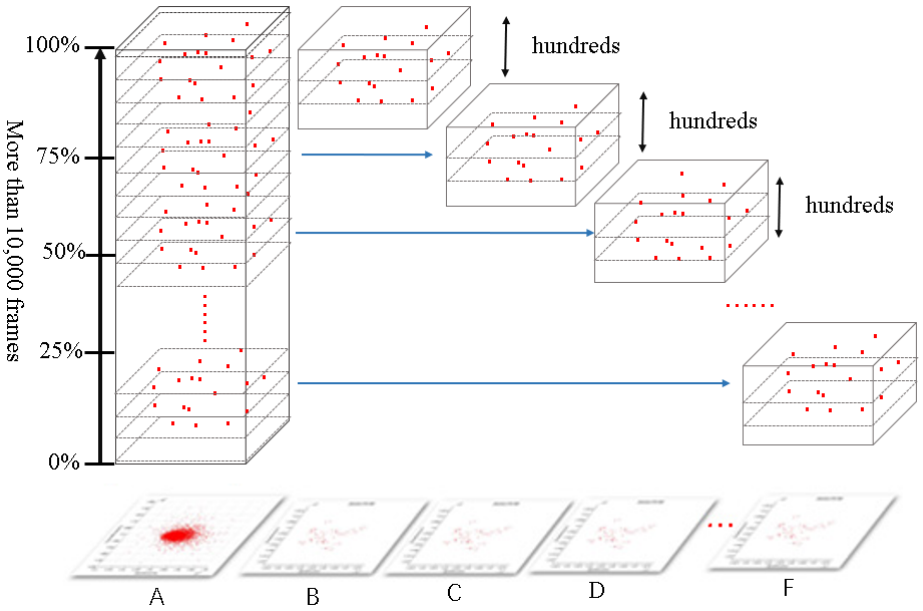

Figure 4.1: The schematic diagram of layering

4.2 Filter isolated fluorescent spots

From a biological perspective, studying the clusters of several fluorescent molecules is a reasonable way to understand the activity of insulin crystals in islet β-cells. The images that have already been processed by Layering process still contain a lot of background-like fluorescent spots which interfere with our judgment. A further process is need to filter these isolate fluorescent spots.

As Figure 4.2 shows, each fluorescent spot will be detected in the image. Draw a circle centered on this fluorescence spot with a radius of several nanometers. Calculate how many spots except itself in this circle. If less than two spots, this fluorescence spot is filtered. If more than or equal to two spots, this spot is retained. For example, the dot in the center of the green circle is retained and the dot in the center of the blue circle is deleted in Fig.4.2. Fig.4.4 shows an example where the right image is filtered from the left one with several obvious clusters. Because this step is necessary, all the images in the result (excluding the result in 4.1), are processed in this way first. Based on the theory 2.4, the distance between two fluorescence spots is 2.2 - 3 nm, which is the reference to set the radius of the circle to 3 nm.

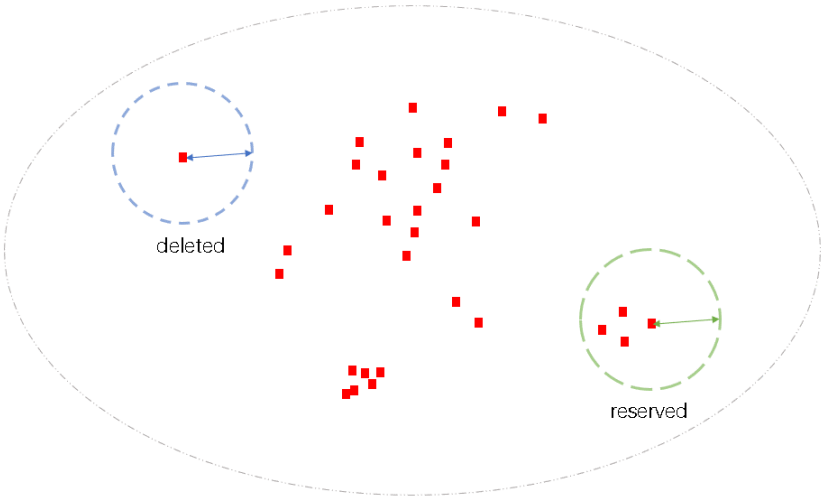

Figure 4.2: The schematic diagram of the filter.

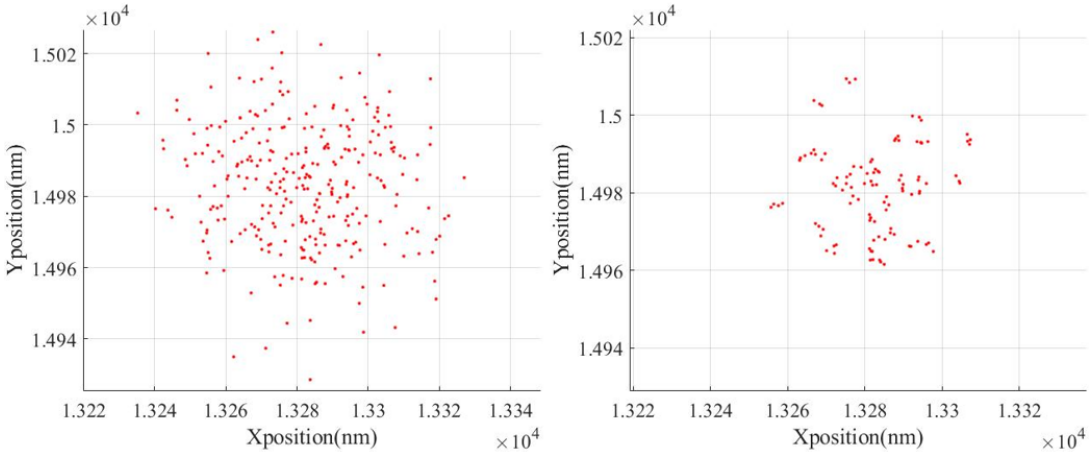

Figure 4.3: The left is the original image and the right one is the processed image, as an example.

4.3 Hypothetical structures

Based on the considerations presented in section 2.4, the insulin crystals in cells are complex and unknown. However, the final form of the insulin crystal in the cell should theoretically have the form of a hexamer. We use the hexamer as a guide to define five hypothetical sub-structures, illustrated in Figure 4.4, which we apply to the image analysis. Due to the positioning variation of each fluorescence spot, we also preset a tolerance for our Hypothetical models. The angle between the three adjacent insulin molecules is 120 ° ± 10°, and the distance between the two fluorescent spots sets as 2.2 to 3 nm accordingly.

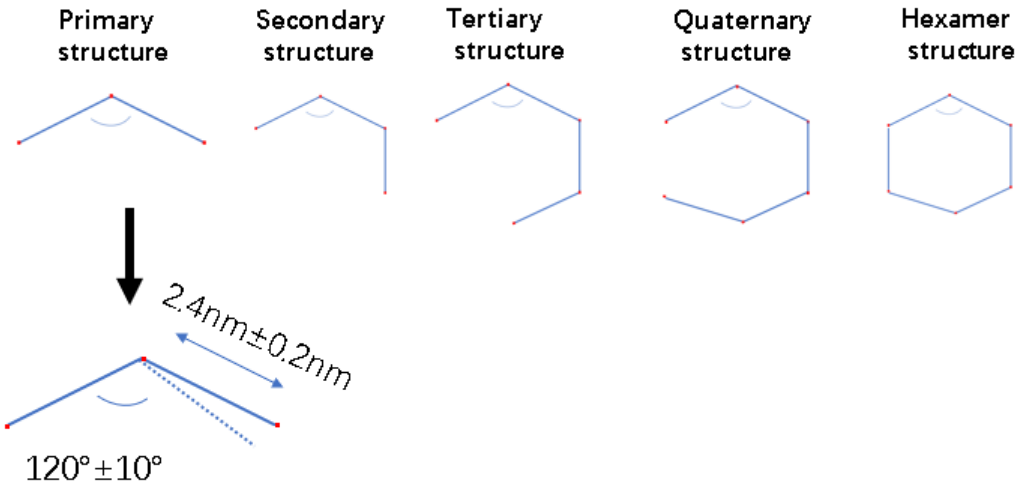

Figure 4.4: The five hypothetical structures in the first row. The second row shows the tolerance of the primary structure.

4.4 Statistic of the distances between all the fluorescent spots

Based on section 2.4, the distance between two fluorescence spots is 2.2 nm-3 nm for an insulin hexamer. Therefore, the statistics of the distances between two fluorescence spots can potentially be interesting to study. The analysis was performed as follows: For each granule of a cell the distances between all fluorescent spots were calculated. The distances were tuned in steps of 0.1 nm and the number in each "bin" was normalized by the number of all spots, i.e.

$$ratio_{distance} = \frac{n_{distance}}{n_{total}} \tag{4.1}$$

where n_{total} is the number of all fluorescence spots, $n_{distance}$ is the number of fluorescence spots fitting one distance.

5

Simulation

For dSTORM microscopy, the accuracy with which the position of a single fluorescent molecule can be obtained is about 10 nm, while the insulin hexamer structure is expected to be on the order of 5 nm. It is therefore not obvious that the presented analysis techniques on actual dSTORM images are capable of identifying the insulin hexamer structures at all. The purpose of the numerical experiments presented in this section is to investigate what localization precision would be needed to ensure that a hexamer identified by the analysis tools is actually real and not just an analysis artefact.

We therefore generated numerical dSTORM images that were analyzed with the same tools as the experimental images. The procedure is illustrated in Figure 5.1. We assume a hexamer with a base length, i.e. the distance between two corners, of 2.4 nm. At each corner a fluorescent molecule is placed. The actual position of the hexamer follows a Gaussian distribution, indicated by the dotted circle. We only consider hexamers oriented parallel to the plane of observation. They can be arbitrarily rotated in that plane. The simulations were performed in Matlab. We focus at the following two aspects:

- How does the accuracy with which the position of a fluorescent molecule can be located influence the probability of the analysis tools to find hexamers in the images?
- Is the assumption of a base length of 2.4 nm for the hexamer realistic?

5.1 Simulation 1

In order to study the effect of localization precision on the probability to identify hexamers with the presented analysis tools, simulated images with different localization precision were produced. Each image includes 33 hexamer and 100 additional random spots equivalent to 298 spots in 50x50nm.

Three representative images are shown in the left column of Figure 5.2. The localization precision of the single fluorescence points of the hexamer in the images (a) (b) (c) are 10 nm, 6 nm and 0 nm, respectively. The results after filtering with the same analysis tools used for the experimental images are shown in the right column of Figure 5.2. It is obvious that hexamers become easier to find with increasing localization precision. Identified hexamers are indicated in blue. Therefore, the

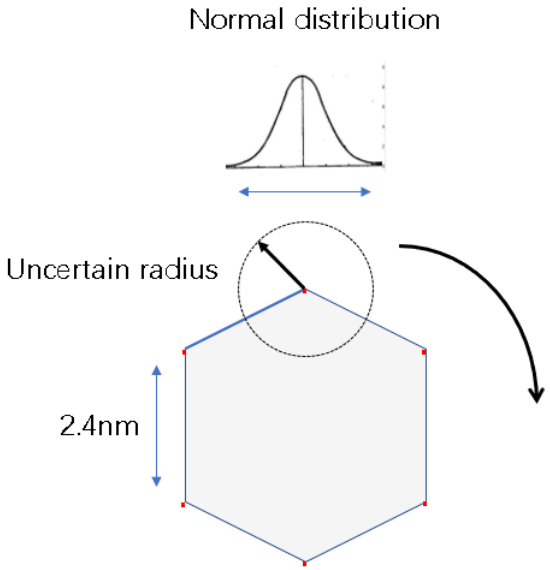

Figure 5.1: The model of a hexamer for the purpose of simulations.

curve for the number of the primary structure versus the localization precision in Figure 5.3 can be obtained. The curve indicates that when the localization precision reaches 1 nm, the structure can be easily identified.

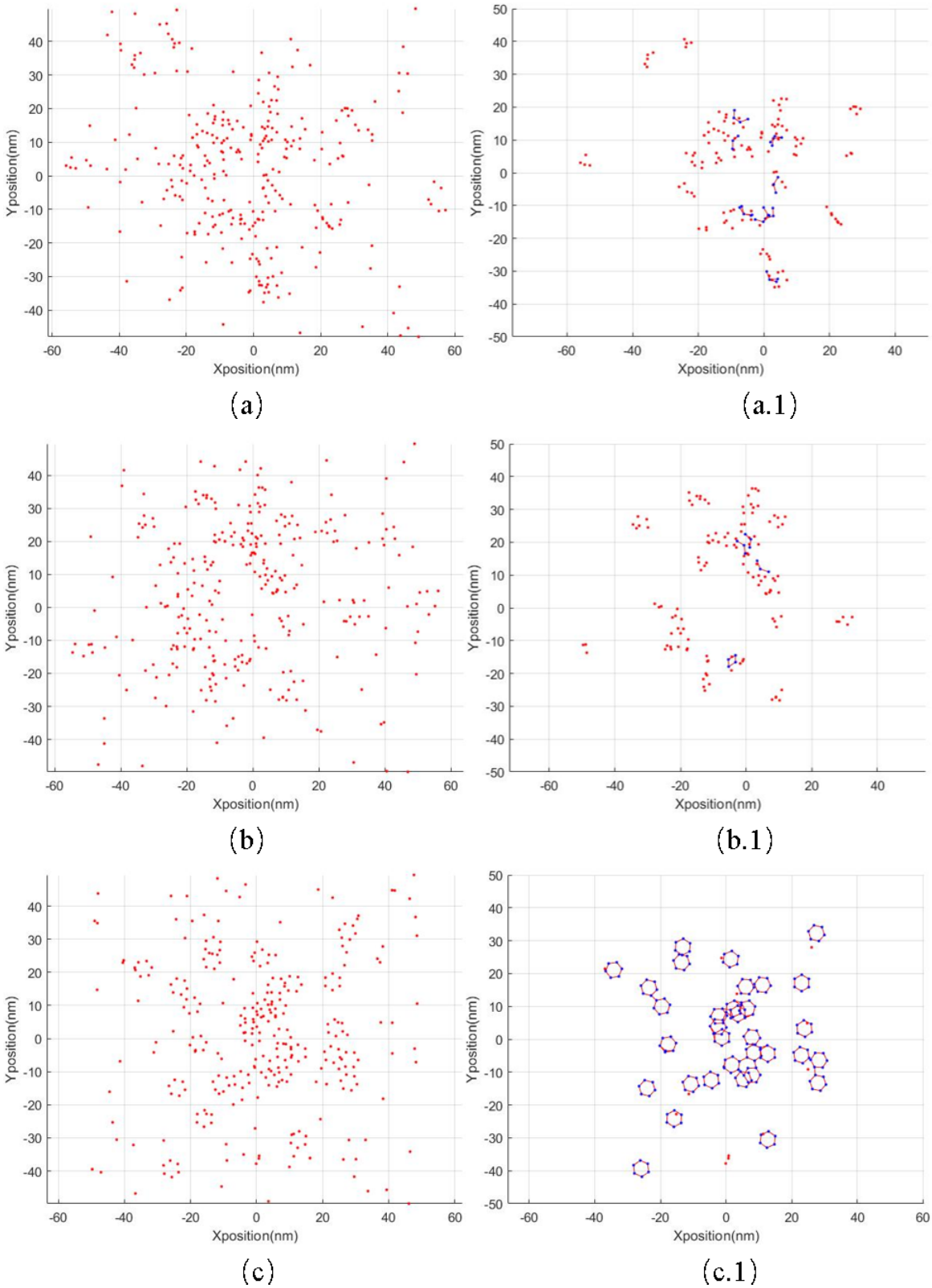

Figure 5.2: From top to bottom, the localization precision of images (a) (b) (c) are 10 nm, 6 nm and 0 nm, respectively. Images (a.1), (b.1) and (c.1) were processed with the same analysis tool as used for the analysis of the experimental images. Hexamers identified by the analysis tool are indicated in blue color.

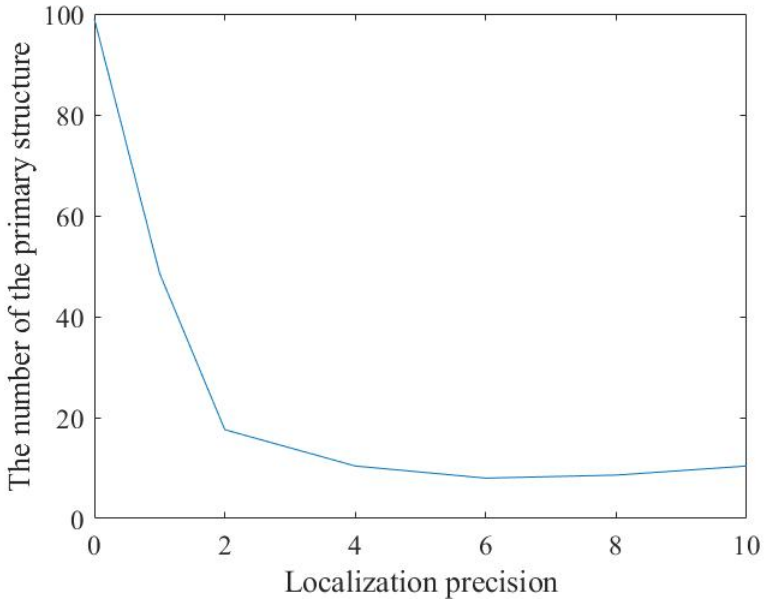

Figure 5.3: The number of the primary structure versus the localization precision.

5.2 Simulation 2

Here, we show simulation results with the purpose of comparing with the analysis of the experimental images presented in section 3.4, where the distance to neighboring fluorescent spots was investigated.

The simulated images contain 90% hexamers (generated the same way as described above) and 10% random spots, which is about 4000 spots in one image as shown in Fig.5.4. In order to be as consistent as possible with the experiment, the overall distribution conforms to the Gaussian distribution. By the way in section 3.4, through the statistic of the distances between all the fluorescent spots , four curves of the result in Fig.5.5 indicate that the peak of 2.4nm value becomes more and more obvious with the improvement of localization precision. Until below 1 nm, the peak of 2.4 nm is very pronounced.

The simulations have all shown above and will be discussed in the section of the conclusion.

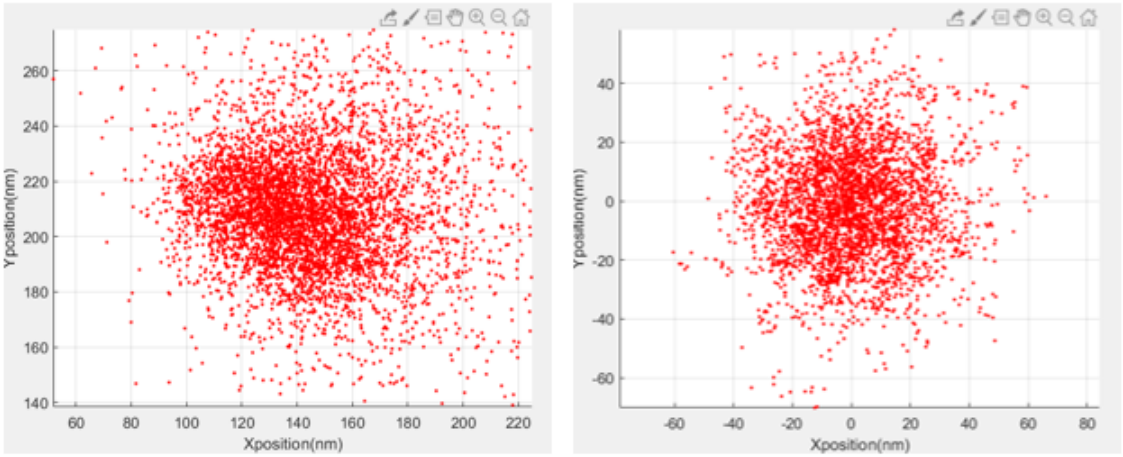

Figure 5.4: Sample image (left) and simulation image (right) in comparison.

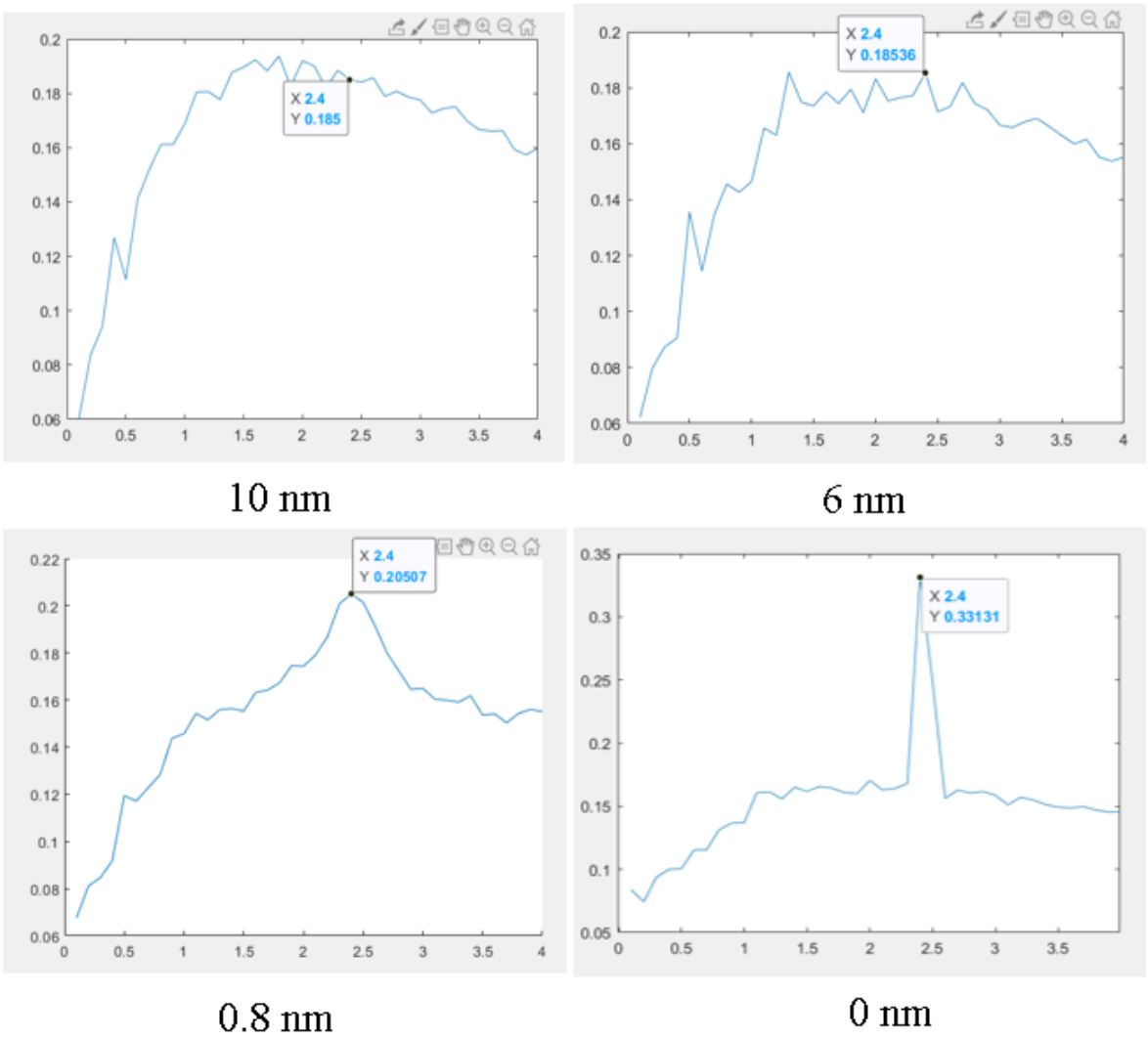

Figure 5.5: The statistic of the distances between all the fluorescent spots with the improvement of localization precision from 10-0 nm.

6

Result and Analysis

6.1 Sub-grouping of dSTORM images

In order to study the substructure of insulin granule, suitable granules which contain enough fluorescent spots have to be distinguished and extracted from a dSTORM image of a complete islet β-cell. Figure 6.1 presents a dSTORM image of one islet β-cell, which was taken by the ELYRA P1 microscope. On the left in Figure 6.1, the dSTORM image was acquired from an islet β-cell that generally shows a thickness of approximately 50 nm and is 25×25 μm. This dSTORM image of islet β-cell is taken about 5 minutes and overlapped by 10000 frames which are shown on the Z axis in the right image.

Interestingly, when zoomed in a certain area on the image (a) of Figure 6.2, we can easily distinguish the clusters which are enriched with high-density fluorescent dots. Then we tried to deeply look on a single cluster we found that a granule-like structure was presented as a reconstructed image (b) or time-series images (c) in Figure 6.2. After review of all the clusters in the cell, we found that the granule-like clusters with 200-300 nm diameter were highly dense and enriched with photon molecules and therefore are selected for further analysis.

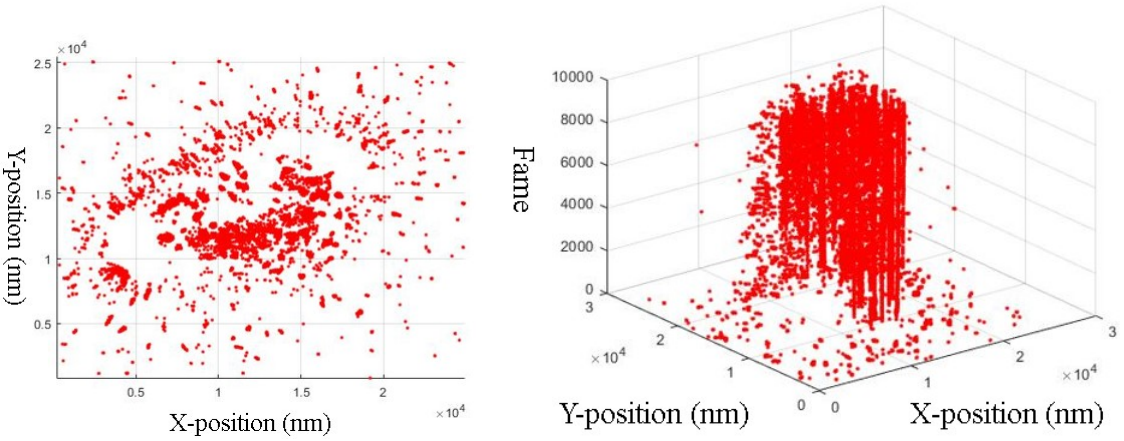

Figure 6.1: dSTORM images of an insulin secreting INS-1 cell. The red spots label excited fluorescent dyes which conjugate with insulin antibodies that indicate insulin molecules located in the cell. The x-y axes present the position of the florescent spots and the z axis presents the time-series frames for both of them. The image on the left is a superposition of all the frames from the image on the right.

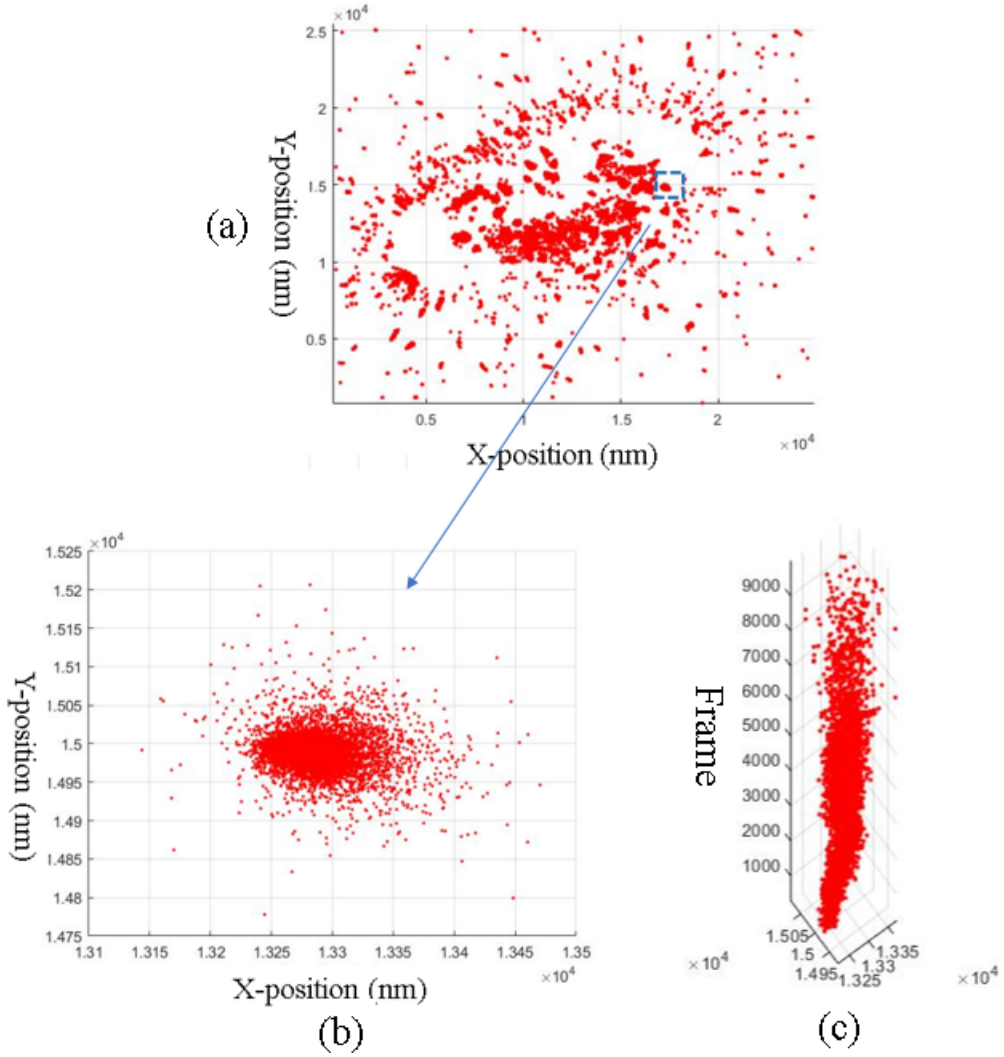

Figure 6.2: Example of how a granule sample was extracted from the complete cell image for further analysis.

6.2 Characterisation of the clusters and structures in the sub-grouped images

As shown in Figure 6.2, it is not constructive to analyze the substructure in the granule based on such a high-density image. Therefore, the images are preprocessed as described in section 4.1. Figure 6.3 shows layered sub-images that were generated by combining 100, 300, 400 and 800 frames, respectively. The densities of fuorescent molecules for the images containing superpositions of 300 frames and 400 frames seem suitable for further analysis. This finding was consistent with images taken of granules of different cells, also showing obvious clusters of fluorescent molecules. These obvious clusters are likely to be rich in biological information which is an interesting target.

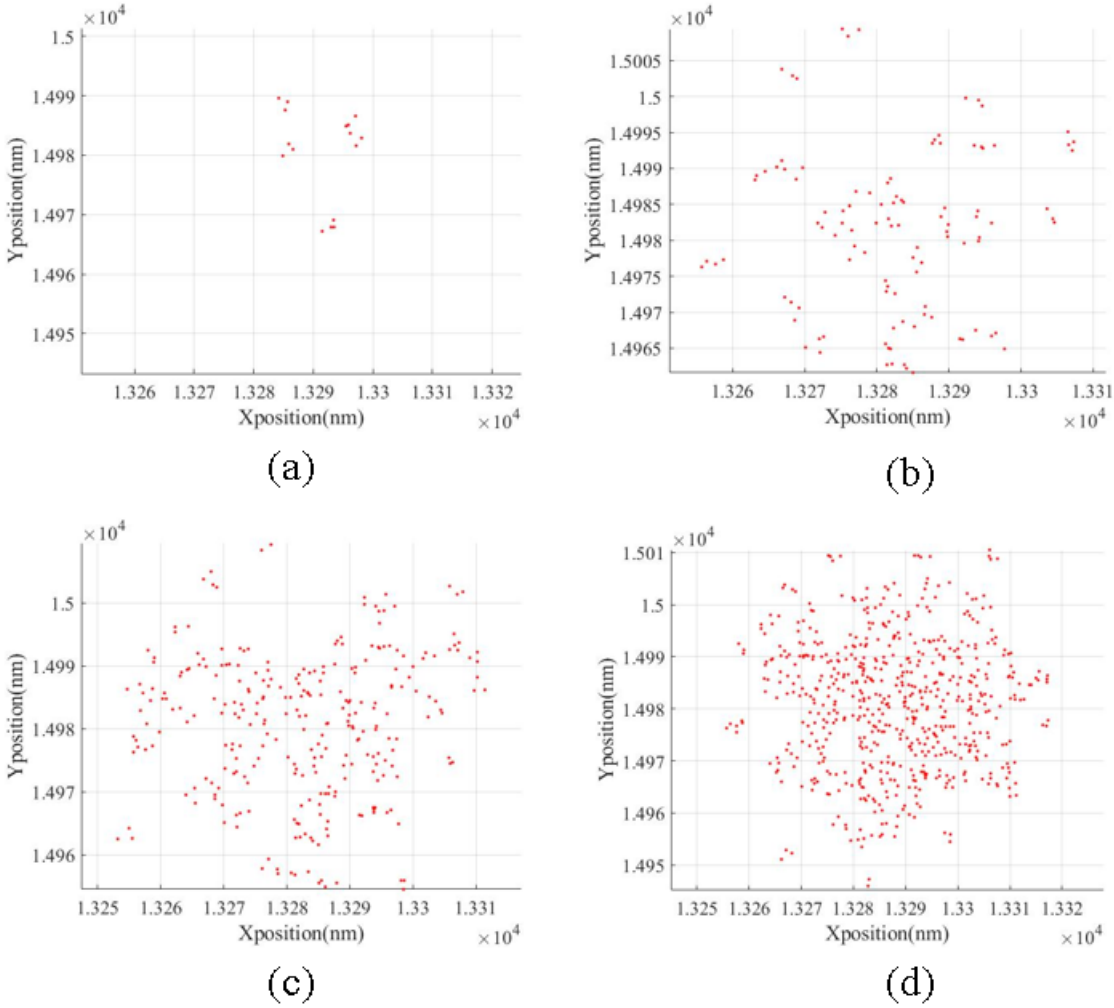

Figure 6.3: The first image (a) is superposition of frames 5000-5100. The second image (b) is superposition of frames 5000-5300. The third image (c) is a superposition of frames 5000-5400. The fourth image (d) is superposition of frames 5000-5800.

In addition, the density of the fluorescent spot is different in the different range of the dSTORM image. Figure 6.4 shows three different examples of 300 combined frames each, i.e. frames 0-300 (a), frames 5000-5300 (b) and frames 7500-7800 (c). As can be seen the density of fluorescent spots is very different for those three selections, indicating that not just the number of combined frames, but also which ranges are combined, is important for preprocessing an image for further analysis. For this study, the density of the spots in the range between 50%-75% is suitable, which is neither rare nor dense.

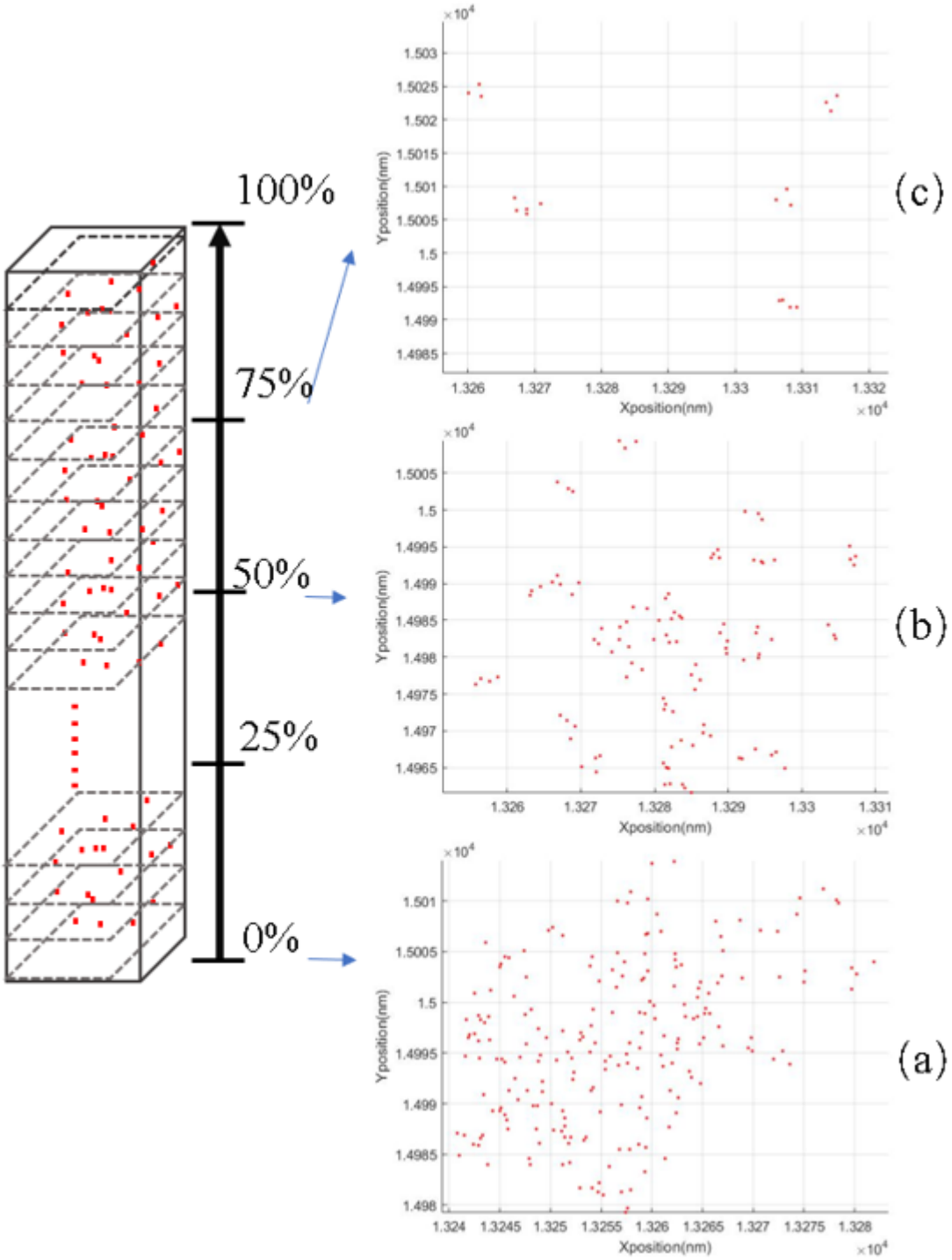

Figure 6.4: The layering parameter is 300 frames per image. The image (a) is a superposition of frames 0-300. The image (b) is a superposition of franes 5000-5300. The image (c) is a superposition of frames 7500-7800. The x-y coordinates are the position coordinates.

6.3 Regulation of distance within trimer

Following the method described in section 4.4, we analyze five different granules from three different cells. The number of fluorescence spots in each granule was an average of about 4000. Figure 6.5 shows the distances between any two points for the five granules. While there are many different peaks in the five curves, only

the peak at 2.4 nm occurred repeatedly in the five different granules. It may be a coincidence. Interestingly, the distance of 2.4 nm belongs to the range of 2.2-3, which may attribute to that the distance between two adjacent corner points of the insulin hexamer corresponds to 2.4 nm.

An identical analysis was performed in section refsimulation 2 for the simulated images. By comparing Figure 6.5 with the simulation results, i.e. Figure 5.5, the trend and shape of the curves for the distances between any two fluorescent points in the experimental images are very close to the simulation results, when a localization precision between 1-10 nm was used. This result indicates that the localization precision of the experiment images could be in the range of 1-10 nm. However, it should be noted that the above is neither a direct evidence of finding insulin hexamers, nor of the size of the hexamer.

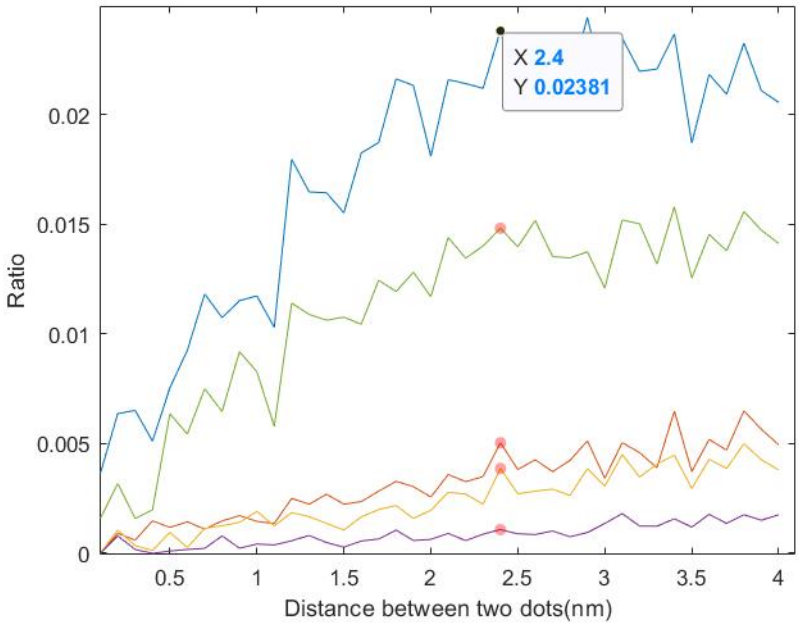

Figure 6.5: Distances between any two spots in one granule. Each curve represents a different granule.

6.4 Trimer structure in sub-grouped images

According to the result of the last section 6.3, we use the distance of 2.4 nm as a standard and set the distance (2.2 to 3 nm) and angle ($120° \pm 10°$) to scan the experimental images as shown in Figure 4.4. Based on the above, we selected three typical images of different granules of different cells. The analysis is summarized in Figure 6.6. Each picture is an overlap of 300 frames. Structures possibly corresponding to insulin hexamers that were identified by the analysis tool are plotted in blue. The percentage of identified structures is given in the table at the bottom of Figure 6.6. The primary structure, i.e. three points that have separation and angle within our parameter interval, can be found regularly in all three samples. About 10% of the fluorescent spots can be associated with the primary structure. The secondary structure, i.e. four points that have separation and angle within our parameter

interval, could only be found in one image and at a lower rate (3.3%). In the images, we can see that many fluorescent spots are clustered together. The structures found by the analysis tool appear in these clusters. Compared to Figure 5.2 and data 5.3 from the simulation, the result is consistent with the situation that the experimentally obtained localization precision seems larger than 1 nm. The simulation indicated that only when the localization precision reaches 1 nm, the hexamer structure will become very visible. Therefore, according to the current localization precision, the results show that it is impossible to identify the hexamer structure in the experimental images.

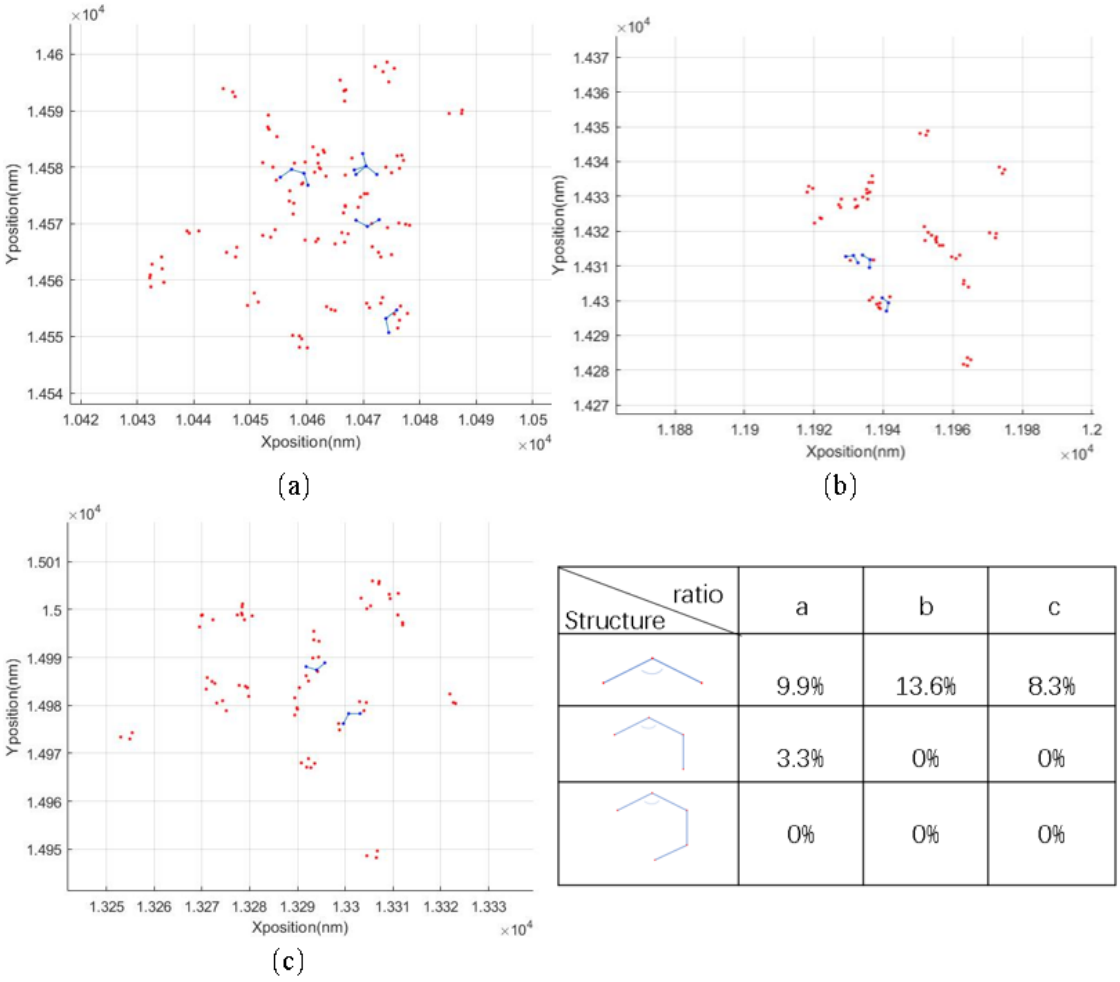

Structure \ ratio	a	b	c
	9.9%	13.6%	8.3%
	3.3%	0%	0%
	0%	0%	0%

Figure 6.6: Three images from three different granules (top row) and the ratio of different structures found by the analysis tool in these three images (bottom table). The x-y coordinates are the position coordinates.

7

Conclusion and plan

7.1 Conclusion

In this work, images of islet β-cell were acquired by dSTORM microscopy. The dye was tagged with the specific insulin antibody that binds to the insulin peptide chain in insulin granules. The positions of the fluorescence spots of the dyes were measured by the dSTORM microscope and the position information of insulin crystal in the cell was therefore obtained. In this way, we can discern the state of the insulin crystals in the cell. In particular, the hypothesis was formulated that the structure of the insulin in the granules has the shape of a hexagon with a size of about 5 nm, i.e. 2.4 nm between two adjacent corners. It should be noted that the size of the hypothetical insulin hexamers is below the localization precision that can be expected from the dSTORM techniques (about 10 nm). Analysis tools were developed to search for hexamers in the experimental images. Simultaneously, simulations were performed to understand how the localisation accuracy would influence the chance to identify insulin hexamers with the developed analysis tools. From this study, we conclude the following:

- By analyzing the reconstructed image and time-series image, single granules which contain high density (>0.3 per nm^2) of the fluorescent spots can be distinguished and extracted from a dSTORM image of entire islet β-cells.
- By layering and filtering the dSTORM image of one granule, cluster-like structures were obtained from the images. The images were processed by selecting 300 to 400 frames from the range between 50% and 75% of a whole image stack consisting of several thousand frames.
- Analysis tools were developed with the goal of identifying the hypothetical insulin hexamers in experimental images. Simplified primary and secondary structures were defined for which the analysis tool scanned the experimental images. For particular images, a few of the primary and secondary structures were obtained. Compared to the section 5.1 results, the result is consistent with the situation that the experiment localization precision is at least greater than 1 nm. The section 5.1 indicated that when the localization precision was less than 1 nm, the hexamer structure would be easily detected. Therefore, it can be concluded that with the current experimental localization precision, the developed analysis tools are not able to explicitly identify the hexamer structure in the experimental images.

- The simplest performed analysis of the experimental images consisted of measuring the distance between any two fluorescent spots in the image. Regularly a peak (however not distinct) at a distance of 2.4 nm was found, which fits well with the expected size of the hypothetical insulin hexamer. However, simulations showed that for the above simple approach to be successful, again the experimental localisation accuracy would need to be below 1 nm.

To summarize, the presented thesis was not able to distinctively identify insulin hexamers in the experimental images. There are however hints that the structures may exist. Simulations have shown that an experimental localisation accuracy of at least 1 nm would be required for the analysis tools developed in this thesis to be able to explicitly identify insulin hexamers in experimental images. From the presented results, we can neither conclude that the hypothetical insulin hexamers exist, nor that they not exist. An explicit answer would either require images with better localisation accuracy or more advanced analysis tools.

8

Acknowledgements

I hereby want to thank my superviser Enming Zhang and my co-superviser Cord Arnold. They helped me a lot with my graduation thesis. Although I was very depressed because of the environmental problems and pressure, they were still very patient to guide my thesis. I am very grateful to them again. I am also grateful for the two years of study and life in Lund university. In these two years, I harvest knowledge and harvest a lot of friendship. Lund university is a place where cultures collide. Here, Here, ideas come into being like sparks, so they are desirable. In a word, I like this town very much. I hope our department will become better and better, and Lund university will become better and better as well.

Bibliography

[1] Economic costs of diabetes in the u.s. in 2012. *Diabetes Care*, 36(4):1033–1046, March 2013.

[2] M. J. Adams, T. L. Blundell, E. J. Dodson, G. G. Dodson, M. Vijayan, E. N. Baker, M. M. Harding, D. C. Hodgkin, B. Rimmer, and S. Sheat. Structure of rhombohedral 2 zinc insulin crystals. *Nature*, 224(5218):491–495, November 1969.

[3] K.G.M.M. Alberti and P.Z. Zimmet and. Definition, diagnosis and classification of diabetes mellitus and its complications. part 1: diagnosis and classification of diabetes mellitus. provisional report of a WHO consultation. *Diabetic Medicine*, 15(7):539–553, July 1998.

[4] MD Ananya Mandal. Insulin chemistry and etymology. https://www.news-medical.net/health/What-is-Insulin.aspx.

[5] E. Betzig, G. H. Patterson, R. Sougrat, O. W. Lindwasser, S. Olenych, J. S. Bonifacino, M. W. Davidson, J. Lippincott-Schwartz, and H. F. Hess. Imaging intracellular fluorescent proteins at nanometer resolution. *Science*, 313(5793):1642–1645, September 2006.

[6] W. Bocian, J. Sitkowski, Elż. Bednarek, A. Tarnowska, R. Kawecki, and L. Kozerski. Structure of human insulin monomer in water/acetonitrile solution. *Journal of Biomolecular NMR*, 40(1):55–64, November 2007.

[7] Ewa Ciszak, John M Beals, Bruce H Frank, Jeffrey C Baker, Nancy D Carter, and G.David Smith. Role of c-terminal b-chain residues in insulin assembly: the structure of hexameric LysB28prob29-human insulin. *Structure*, 3(6):615–622, June 1995.

[8] U Derewenda, Z Derewenda, G G Dodson, R E Hubbard, and F Korber. Molecular structure of insulin: The insulin monomer and its assembly. *British Medical Bulletin*, 45(1):4–18, 1989.

[9] B. Huang, W. Wang, M. Bates, and X. Zhuang. Three-dimensional super-resolution imaging by stochastic optical reconstruction microscopy. *Science*, 319(5864):810–813, February 2008.

[10] Irene Krämer and Thomas Sauer. The new world of biosimilars: what diabetologists need to know about biosimilar insulins. *The British Journal of Diabetes & Vascular Disease*, 10(4):163–171, July 2010.

[11] Jackson Immuno Research Europe Ltd. Alexa fluor 647 technical information. https://www.jacksonimmuno.com/technical/products/conjugate-selection/alexa-fluor/647.

[12] World Health Organization. Diabetes fact sheet n312. https://www.who.int/en/news-room/fact-sheets/detail/diabetes.

[13] James B. Pawley, editor. *Handbook Of Biological Confocal Microscopy*. Springer US, 2006.

[14] Michael J Rust, Mark Bates, and Xiaowei Zhuang. Sub-diffraction-limit imaging by stochastic optical reconstruction microscopy (STORM). *Nature Methods*, 3(10):793–796, August 2006.

[15] Jakob Suckale and Michele Solimena. The insulin secretory granule as a signaling hub. *Trends in Endocrinology & Metabolism*, 21(10):599–609, October 2010.

[16] Sune Svanberg. *Atomic and Molecular Spectroscopy*. Springer Berlin Heidelberg, 2004.

[17] Russell E. Thompson, Daniel R. Larson, and Watt W. Webb. Precise nanometer localization analysis for individual fluorescent probes. *Biophysical Journal*, 82(5):2775–2783, May 2002.

[18] E. Vanea, C. Gruian, C. Rickert, H.-J. Steinhoff, and V. Simon. Structure and dynamics of spin-labeled insulin entrapped in a silica matrix by the sol–gel method. *Biomacromolecules*, 14(8):2582–2592, July 2013.

[19] Tine N. Vinther, Mathias Norrman, Holger M. Strauss, Kasper Huus, Morten Schlein, Thomas Å. Pedersen, Thomas Kjeldsen, Knud J. Jensen, and František Hubálek. Novel covalently linked insulin dimer engineered to investigate the function of insulin dimerization. *PLoS ONE*, 7(2):e30882, February 2012.

[20] Ian M. Williams, Francisco A. Valenzuela, Steven D. Kahl, Doraiswami Ramkrishna, Adam R. Mezo, Jamey D. Young, K. Sam Wells, and David H. Wasserman. Insulin exits skeletal muscle capillaries by fluid-phase transport. *Journal of Clinical Investigation*, 128(2):699–714, January 2018.

[21] ZEISS. Zeiss elyra 7 with lattice sim. https://www.zeiss.com/microscopy/int/products.